SEMARAK ILMU PUBLISHING

Journal of Advanced Research in Fluid Mechanics and Thermal Sciences

Journal homepage:
https://semarakilmu.com.my/journals/index.php/fluid_mechanics_thermal_sciences/index
ISSN: 2289-7879

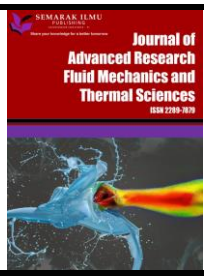

The Influence of Variable Fluid Properties on Peristaltic Transport of Eyring Powell Fluid Flowing Through an Inclined Uniform Channel

Balachandra Hadimani[1], Rajashekhar Choudhari[2], Prathiksha Sanil[1], Hanumesh Vaidya[3], Manjunatha Gudekote[1,*], Kerehalli Vinayaka Prasad[3], Jyoti Shetty[2]

[1] Department of Mathematics, Manipal Institute of Technology, Manipal Academy of Higher Education, Manipal, India
[2] Department of Mathematics, Manipal Institute of Technology Bengaluru, Manipal Academy of Higher Education, Manipal, India
[3] Department of Mathematics, Vijayanagara Sri Krishnadevaraya University, Ballari, India

ARTICLE INFO

Article history:
Received 10 August 2022
Received in revised form 24 December 2022
Accepted 4 January 2023
Available online 24 January 2023

Keywords:
Peristaltic mechanism; variable viscosity; variable thermal conductivity; inclination; Eyring-Powell fluid

ABSTRACT

The current study emphasises a new approach to the peristaltic transport of Eyring-Powell fluid through a uniform channel. The study is done while considering the influence of variable liquid properties and wall properties through a uniform inclined channel, and the flow problem is developed mathematically. The study uses low Reynolds number and long-wavelength approximations to simulate no-slip conditions on the channel walls. The solutions are derived using a traditional double perturbation technique, and the nonlinear governing equations are normalized by employing pertinent non-dimensional factors. Graphical representations of the impact of significant physical parameters, such as velocity, temperature, concentration, and streamlines, are depicted and discussed. It was noted that Eyring-Powell fluid parameters and variable liquid properties have major impact during the peristalsis.

1. Introduction

Peristalsis is a natural mechanism in the human body that causes a gradual wave of regional muscular contractions and relaxations and is responsible for numerous biological processes such as food flow through the esophagus and ovum migration in the female uterine tube. Because of its use in biomedical and industrial purposes, peristaltic motion of non-Newtonian and viscous fluids has been researched in recent decades. Latham [1] initiated the study on peristaltic urine flow via the ureter and determine fluid flow velocity and pressure for various flow rates using Newtonian compressible fluid. The peristaltic mechanism was later studied by Shapiro *et al.,* [2] under circumstances like long wavelength and low Reynolds number. The same conditions are being used to date. Raju and Devanathan [3] investigated the effect of applied pressure and non-Newtonian parameter on the velocity and streamlines of a power-law fluid under various conditions. Srivastava *et al.,* [4] studied the peristalsis of physiological fluid, flowing in a non-uniform axisymmetric tube

* *Corresponding author.*
E-mail address: manjunatha.g@manipal.edu; gudekote_m@rediffmail.com

https://doi.org/10.37934/arfmts.102.2.166185

with constant and variable viscosity. Usha and Ramachandran [5] explored the peristaltic transport of two-layered Power Law fluid. They studied the effect of shear thinning and shear thickening in the fluid's core and peripheral layer in an axisymmetric tube. Further, Vajravelu *et al.,* [6] focused on studying the peristaltic motion of Hershel-Bulkley liquid in the channel, which warrants the study of fluid flow characteristics.

In biofluid dynamics, the no-slip criterion for viscous fluids proposes the liquid always moves at a constant speed relative to the boundary of a solid wall. The fluid velocity equals the solid edge velocity at all fluid-solid interfaces. One could imagine the fluid's outermost molecules sticking to the surfaces it passes through. Driven by this application, Hayat *et al.,* [7] investigated the Soret and Dufour effect on the peristaltic flow of Prandtl fluid. They considered compliant tube walls and no-slip conditions were applied for equation of momentum, energy, and concentration. As a result, they concluded that the large Soret and Dufour number activates the temperature while reducing the concentration. In a further study conducted by Hayat *et al.,* [8] on hyperbolic tangent nanofluid under similar conditions with MHD, it was noticed that temperature increases for higher Brownian movement and thermophoresis parameters. As of late Vaidya *et al.,* [9] investigated the peristaltic motion of Rabinowitsch fluid in an inclined channel with compliant walls. The series perturbation technique is utilised to solve the non-dimensional governing equations, and the streamlines were analyzed.

This research is crucial when it comes to an understanding of how heat moves through biological fluids. Conduction, radiation, convection, and evaporation all play a role in keeping the body's temperature stable. Sobh [10] investigated the interplay between peristaltic motion and heat transfer in viscous fluid flow by considering the impacts of heat transfer in a stable transverse magnetic field. During their research, it was noticed that the heat transfer coefficient at the channel walls varied depending on the kind of channel. According to the study, as the Hartmann number grows, so does the heat transmission rate. The heat transfer coefficient behaves the same for both non-uniform and uniform channels in heat transmission. Ali *et al.,* [11] also investigated peristaltic transport in a curved channel. The heat transmission rate is slower in a curved channel than in a straight channel. Prandtl fluid peristalsis in the presence of MHD flow was studied by Alsaedi *et al.,* [12]. The perturbation approach is used to get series solutions for physical parameters such as velocity and temperature. The Hartmann number was shown to be a decreasing function of heat transport. Through slip effects, Bhatti and Zeeshan [13] examine how heat and mass transfer affect particle-fluid suspension produced by peristaltic transit. For the embedded particles in Casson fluid model, the non-dimensional governing equations of the fluid and particulate phase are interpreted on the premise of a long-wavelength approximation and disregarding inertial forces. The study's findings warrant an inquiry into various types of non-Newtonian and Newtonian fluids. According to Vaidya *et al.,* [14], the MHD peristalsis of Bingham fluid via a uniform channel is affected by wavelength and Reynolds number. It is shown that the temperature profile becomes more consistent as the value of variable thermal conductivity rises, even while considering heat transmission and wall features. Manjunath *et al.,* [15] investigated how thermal conductivity and heat transfer influenced Jeffery fluid peristaltic flow in an inclined elastic tube with porous walls. It is clear from the data that lowering the Biot number lowers the temperature. The main goal of the study by Sandhya Rani et al., [16] is to address mass and heat transfer across electro-hydrodynamics by considering Cattaneo-Christov model. When a blood-based hybrid nanofluid flows over a vertical stretchy area, the Lorentz force is applied. The Cattaneo-Christov model theories were examined using thermal radiation that can generate heat.

In a porous medium, researchers Kodantapani and Srinivas [17] looked at the impact of wall characteristics on MHD peristalsis and heat transport. The increase in rigidity and stiffness

parameters was seen to increase velocity and temperature. At the same time, the damping properties of the wall are decreasing. Hayat and Hina [18] studied the impact of MHD and compliant walls on Maxwell fluid peristalsis. The effect of wall compliance on Burgers' fluid peristalsis was studied by Mariyam *et al.,* [19]. Increases in wall tension, rigidity, and stiffness increase velocity, whereas increases in wall damping lead to an increase in speed in a non-uniform channel with wall characteristics and heat transfer. The peristaltic wave propagation of non-Newtonian Casson liquid was studied by Devaki *et al.,* [20]. According to these studies, the larger the flow pattern and the greater the number of boluses, the more rigid and stiff the wall becomes. Using a non-uniform inclined tube with a long wavelength and a short Reynold's number, Manjunath *et al.,* [21] investigate the effects of slip and wall qualities on the peristaltic transport of Rabinowitsch fluid. Newtonian and pseudoplastic liquid models have been proposed. When the rigidity and stiffness parameter values rise, the volume of trapped bolus grows; however, when the viscous damping force parameter values increase, the volume decreases, as they discovered in their research.

The processes influencing blood flow in tiny arteries and ducts, lymphatic vessels, and the intestines have not been studied in studies on physiological fluids with continuous liquid properties. Most older studies used constant heat conductivity and viscosity as their guiding principles. The viscosity and heat conductivity have a considerable impact on biological fluids. Casson fluid peristaltic movement in a convectively heated inclined porous tube was studied by Rajashekhar *et al.,* [22] using changing viscosity and thermal conductivity. Thermal conductivity and viscosity were considered in their investigation. Analysis of the impact of factors on physiological variables was done by plotting graphs. Velocity profiles may be improved by altering the viscosity of the fluid. Under the impact of varying fluid characteristics and convective heat transmission, the peristaltic process of Rabinowitsch liquid in a small porous channel is examined by Vaidya *et al.,*[23]. Further, the peristalsis of Rabinowitsch fluid via a nonuniform tube is studied by Vaidya *et al.,* [24] in relation to variations in viscosity and thermal conductivity. Consideration is given to the wall characteristics and convective surface conditions. Long wavelength and low Reynolds number approximations are used to solve the dimensionless governing equations of motion, momentum, and energy. Jeffery fluid peristaltic flow in a channel with variable fluid properties is the subject of research by Manjunatha *et al.,* [25]. Coefficient of variable viscosity increases velocity, Nusselt number, and temperature fields in the study but has the opposite effect on concentration profiles, according to the results. MHD peristalsis flow across a porous channel with varying liquid characteristics and convective circumstances was studied by Vaidya *et al.,* [26]. The analyses by Divya *et al.,* [27] take into account the mass and heat transport characteristics of the Casson fluid, using convective boundary conditions and taking into account how the thermal conductivity changes with fluid temperature. Ree-Eyring fluids may be peristaltic flow through a homogeneous compliant tube with varying viscosity and thermal conductivity, according to Rajashekhar *et al.,* [28]. According to the findings, a Newtonian fluid has a higher velocity than a non-Newtonian fluid. Vaidya *et al.,* [29] studied the peristaltic motion of Ree-Eyring in an inclined permeable channel, where both homogeneous and heterogeneous chemical reactions were observed. Tiny artery convective and wall features were considered in the research, which concentrated on simulating blood flow in small arteries. Karem Mahmoud Ewis [30] investigates and discusses the impact of porosity, varying thermal conductivity, and the Grashof number on the heat transmission and natural convection of viscoelastic fluid flow.

A novel mathematical model of the impact of mass and heat transfer on the peristaltic transport of Eyring–Powell fluid was recently created by Akbar *et al.,* [31]. When Noreen and Qasim [32] examined Eyring Powell fluid peristalsis in a channel under an induced magnetic field, the fluid characteristics of Eyring-Powell liquid showed the opposite behavior. Eyring–Powell fluid peristaltic transport in a heat/mass transmission channel was studied by Hina [33]. The combined effects of slip

and MHD were examined. There were considerations for the effects of viscous dissipation in the study. The heat transfer coefficient is inversely proportional to the parameters of the magnetic field and the velocity slip. The impact of a magnetic field in radial direction on Eyring–Powell liquid peristalsis in a curved conduit was studied by Farooq *et al.,* [34]. Peristaltic transport of Eyring-Powell fluid with electro-kinetic pumping and a transverse Lorentz force was recently explored by Mabood *et al.,* [35]. Electro-Osmosis impedance dependence on surface roughness and induced magnetic field was studied by Asha and Namrata [36] in the Peristalsis of Eyring Powell nanofluid in an asymmetric tapered channel.

To the best of the author's knowledge, the research on the peristalsis of Eyring-Powell fluid in an inclined uniform channel under variable liquid characteristics and wall properties has not been carried out in the literature. The governing nonlinear equations made simpler using approximations with a large wavelength and a low Reynolds number. The governing equations are then solved using the conventional Perturbation approach. The present attempt has been undertaken to overcome this knowledge gap in the Eyring Powell fluid with heat and mass transport and variable liquid properties.

2. Formulation of the Problem

Consider a viscous incompressible fluid flowing through an inclined uniform axisymmetric channel (see Figure 1). Non-Newtonian Eyring-Powell fluid governs the flow. The equations governing the flow [9] are written as follows

$$\frac{\partial u'}{\partial x'} + \frac{\partial w'}{\partial y'} = 0 \tag{1}$$

$$\rho\left[\frac{\partial w'}{\partial t'} + u'\frac{\partial w'}{\partial x'} + w'\,\frac{\partial w'}{\partial y'}\right] = -\frac{\partial p'}{\partial x'} + \frac{\partial \tau'_{x'x'}}{\partial x'} + \frac{\partial \tau'_{x'y'}}{\partial y'} + \rho g \sin\alpha \tag{2}$$

$$\rho\left[\frac{\partial u'}{\partial t'} + u'\,\frac{\partial u'}{\partial x'} + w'\frac{\partial u'}{\partial y'}\right] = -\frac{\partial p'}{\partial y'} + \frac{\partial \tau'_{x'y'}}{\partial x'} + \frac{\partial \tau'_{y'y'}}{\partial y'} + \rho g\ \cos\alpha \tag{3}$$

$$\rho C_P\left[\frac{\partial T'}{\partial t'} + u'\frac{\partial T'}{\partial x'} + w'\frac{\partial T'}{\partial y'}\right] = k_1\left[\frac{\partial}{\partial x'}\left(k(T')\frac{\partial T'}{\partial x'}\right) + \frac{\partial}{\partial y'}\left(k(T')\frac{\partial T'}{\partial y'}\right)\right] + \tau'_{x'x'}\ \frac{\partial u'}{\partial x'} + \tau'_{y'y'}\ \frac{\partial w'}{\partial y} + \tau'_{x'y'}\left(\frac{\partial u'}{\partial x'} + \frac{\partial w'}{\partial y'}\right) \tag{4}$$

$$\left[\frac{\partial C'}{\partial t'} + u'\frac{\partial C'}{\partial x'} + w'\frac{\partial C'}{\partial y'}\right] = D\left[\frac{\partial^2 C'}{\partial x^2} + \frac{\partial^2 C'}{\partial y^2}\right] + \frac{DK_T}{T_m}\left[\frac{\partial^2 T'}{\partial x^2} + \frac{\partial^2 T'}{\partial y^2}\right] \tag{5}$$

where u' and w' are the velocity components in radial direction and axial direction respectively. ρ is the constant fluid density, p' is the pressure, $\tau'_{x'x'}$, $\tau'_{x'y'}$, $\tau'_{y'y'}$ are the extra stress components. While k_1, T', C_P denotes mass diffusivity coefficient, temperature, and the specific heat at constant volume, respectively.

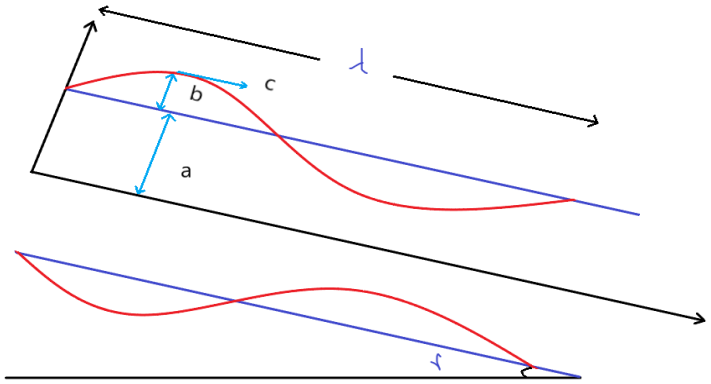

Fig. 1. Physical model

The boundary conditions for the problem [9] are as follows

$$\psi' = \frac{F}{2}, \quad \frac{\partial^2 \psi'}{\partial y'^2} = 0, \frac{\partial T'}{\partial y'} = 0, \quad \frac{\partial C'}{\partial y'} = 0 \quad at \quad y' = 0, \tag{6}$$

$$\frac{\partial \psi'}{\partial y'} = -c\,, T' = T'_1\,, C' = C'_1 \;\; at \;\; y' = H' = a' + b' \sin\left(\frac{2\pi}{\lambda}\,(x' - ct')\right) \tag{7}$$

where λ is the wavelength, a' is the radius of the channel, b' is the wave amplitude, and t' is the time. We now introduce the dimensionless quantities:

$$x = \frac{x'}{\lambda}\,, y = \frac{y'}{a'}\,, w = \frac{w'}{c}\,, u = \frac{\lambda u'}{ca}\,, \tau_{xx} = \frac{a'\tau'_{x'x'}}{c\,\mu}\,, \tau_{xy} = \frac{a'\tau'_{x'y'}}{c\,\mu}, \tau_{yy} = \frac{a'\tau'_{y'y'}}{c\,\mu}\,, \vartheta = \frac{\mu_0}{\rho},$$

$$t = \frac{c\,t'}{\lambda}\,,\; \psi = \frac{\psi'}{ac}\;\; , Re = \frac{a\,c\,\rho}{\mu}\,, p = \frac{a'^2 p'}{c\,\lambda\,\mu}\;\; , \epsilon = \frac{b'}{a'}\,, \theta = \frac{T' - T'_0}{T'_0}\,, Sr = \frac{\rho D K_T (T' - T'_0)}{T_m C'_0}, Sc = \frac{\mu}{\rho D}\,,$$

$$Pr = \frac{\mu\, C_P}{k_1}\;\; , \delta = \frac{a'}{\lambda}\;,\; \mu'_0 = \frac{\mu_0}{\mu}\,, F = \frac{\vartheta c}{g a'^2}\;,\; Ec = \frac{c^2}{\delta T_0},\; Br = Ec.Pr,\; \sigma = \frac{C' - C'_0}{C'_0}\;,\; E_1 = -\frac{\tau a'^3}{\lambda \mu_0^3 c},$$

$$E_2 = \frac{m_1\, a'^3 c}{\lambda^3 \mu_0}\,, E_3 = \frac{m_2 a'^3}{\lambda^3 \mu}, E_4 = \frac{m_3 a'^3}{\lambda^5 \mu_0 c},\; E_5 = \frac{Ha'^3}{\lambda \mu_0\, c}\,, h = \frac{H'}{a'} = 1 + \epsilon \sin\big(2\pi(x - t)\big) \tag{8}$$

Using Eq. (8) in Eqs. (1-7) and by applying the long wavelength and low Reynolds number approximations, we get the non-dimensional governing equations of the form as below:

$$\frac{\partial p}{\partial x} = \frac{\partial\, \tau_{xy}}{\partial y} + \frac{\sin\gamma}{F}, \tag{9}$$

$$\frac{\partial p}{\partial y} = 0, \tag{10}$$

$$\frac{\partial}{\partial y}\left(k(\theta)\,\frac{\partial \theta}{\partial y}\right) + Br\,\tau_{xy}\frac{\partial^2 \psi}{\partial y^2} = 0, \tag{11}$$

$$\frac{\partial^2 \phi}{\partial y^2} + ScSr\frac{\partial^2 \theta}{\partial y^2} = 0, \tag{12}$$

where Br is the Brinkman number and τ_{xy} is the constitutive equation of Eyring Powell fluid [31] given by

$$\tau_{xy} = \{\mu(y) + B\}\ \frac{\partial^2 \psi}{\partial y^2} - \frac{A}{3}\left(\frac{\partial^2 \psi}{\partial y^2}\right)^3. \tag{13}$$

The corresponding dimensionless boundary conditions for Eq. (6) and (7) are

$$\psi = \frac{F}{2}, \quad \frac{\partial^2 \psi}{\partial y^2} = 0, \quad \frac{\partial \theta}{\partial y} = 0,\ \frac{\partial \phi}{\partial y} = 0 \quad at \quad y = 0, \tag{14}$$

$$\frac{\partial \psi}{\partial y} = -1,\ \theta = 1,\ \phi = 1,\ at \quad y = h. \tag{15}$$

The variable fluid properties are given by the following relations

$\mu(y) = 1 - \alpha y$, for α << 1,
$k(\theta) = 1 + \beta\theta$, for β << 1.

where α is the coefficient of variable viscosity, and β is the coefficient of variable thermal conductivity.

3. Results

The Eq. (9) and (11) are nonlinear differential equations hence, an analytical solution for these equations is not possible. Therefore, we introduce the series solution using the double perturbation technique to obtain the solutions.

$$\psi = \Sigma A^n \psi_n, \tag{16}$$

$$\theta = \Sigma A^n \theta_n, \tag{17}$$

By ignoring the higher order terms, we obtain the streamline function as given below

$$\psi = \psi_0 + A\,\psi_1, \tag{18}$$

Applying the Eq. (18) in Eq. (9) and (13), we obtain the following.

$$(P - f)\ y = \{1 - \alpha_1 y + B\}\ \frac{\partial^2 \psi_0}{\partial y^2}, \tag{19}$$

$$\{1 - \alpha y + B\}\ \frac{\partial^2 \psi_1}{\partial y^2} - \frac{1}{3}\left(\frac{\partial^2 \psi_0}{\partial y^2}\right)^3 = 0, \tag{20}$$

$$\psi_0 = \frac{F}{2},\ \frac{\partial^2 \psi_0}{\partial y^2} = 0 \text{ at } y = 0 \text{ and } \frac{\partial \psi_0}{\partial y} = -1 \text{ at } y = h, \tag{21}$$

$$\psi_1 = 0, \quad \frac{\partial^2 \psi_1}{\partial y^2} = 0 \quad at \ \ y = 0 \ \text{ and } \ \frac{\partial \psi_1}{\partial y} = 0 \quad \text{at } \ y = h. \tag{22}$$

Similarly, by ignoring the higher order terms in Eq. (17), we obtain, temperature expression as

$$\theta = \theta_0 + \beta \theta_1, \tag{23}$$

By applying Eq. (23) in Eq. (11), we obtain the following

$$\frac{\partial \theta_0}{\partial y} + \beta \theta_0 \frac{\partial \theta_0}{\partial y} + C_1 = 0, \tag{24}$$

$$\frac{\partial \theta_1}{\partial y} + \beta \theta_0 \frac{\partial \theta_1}{\partial y} + \beta \theta_1 \frac{\partial \theta_0}{\partial y} + C_2 = 0, \tag{25}$$

$$\frac{\partial \theta_0}{\partial y} = 0 \text{ at } y = 0 \ \text{ and } \theta_0 = 1 \text{ at } y = h, \tag{26}$$

$$\frac{\partial \theta_1}{\partial y} = 0 \text{ at y} = 0 \text{ and } \ \theta_1 = 0 \text{ at } y = h. \tag{27}$$

The above equations are nonlinear; hence, we apply the double perturbation technique to obtain the solutions.

$$\psi_i = \Sigma \alpha^j \psi_{ij} \text{ where } 0 \le j \le n \, , \tag{28}$$

$$\theta_i = \Sigma \, \beta^j \, \theta_{ij} \text{ where } \ 0 \le j \le n. \tag{29}$$

We ignore $O(\alpha^2)$ and $O(\beta^2)$ to obtain a more straightforward solution for streamline function and temperature. Then we obtain the streamline function for zeroth order as,

$$\psi_0 = \ \psi_{00} + \alpha \psi_{01}, \tag{30}$$

where,

$$\psi_{00} = \frac{(P-f)y^3}{6(1+B)} + y\left(-1 - \frac{(P-f)h^2}{2(1+B)}\right) + \frac{F}{2}, \tag{31}$$

$$\psi_{01} = \frac{(P-f)y^4}{12(1+B)^2} - \frac{(P-f)h^3}{3(1+B)^2} y. \tag{32}$$

Similarly, we obtain the streamline function for first order as,

$$\psi_1 = \ \psi_{10} + \alpha \psi_{11}, \tag{33}$$

where,

$$\psi_{10} = \frac{(P-f)^3 y^5}{60(1+B)^4} - \frac{(P-f)^3 h^4}{12(1+B)^4} y, \tag{34}$$

$$\psi_{11} = \frac{4(P-f)^3 y^6}{90(1+B)^5} - \frac{4(P-f)^3 h^5}{15(1+B)^5} y. \tag{35}$$

The solution for temperature through the double perturbation technique for zeroth order is given by

$$\theta_0 = \theta_{00} + \beta\theta_{01}, \tag{36}$$

where,

$$\theta_{00} = Q_1 - Q_2 + 1, \tag{37}$$

$$\theta_{01} = Q_3 + Q_5 + Q_7 + Q_9 - Q_4 - Q_6 - Q_8 - Q_{10} - Q_1(1 - Q_2) + Q_2(1 - Q_2). \tag{38}$$

Similarly, we obtain temperature expression for first order as,

$$\theta_1 = \theta_{10} + \beta\theta_{11}, \tag{39}$$

where,

$$\theta_{10} = Q_{11} - Q_{12}, \tag{40}$$

$$\theta_{11} = -(Q_1 + 1 - Q_2)(Q_{11} - Q_{12}). \tag{41}$$

The analytical solution for the velocity can be obtained using the formula, $u = \frac{\partial \psi}{\partial y}$. Therefore, velocity

$$u = \frac{(P-f)y^2}{2(1+B)} - \frac{(P-f)h^2}{2(1+B)} + \alpha\left(\frac{(P-f)y^3}{3(1+B)^2} - \frac{(P-f)h^3}{3(1+B)^2}\right) + A\left(\frac{(P-f)^3 y^4}{12(1+B)^4} - \frac{(P-f)^3 h^4}{12(1+B)^4}\right) + A\,\alpha\left(\frac{4(P-f)^3 y^5}{15(1+B)^5} - \frac{4(P-f)^3 h^5}{15(1+B)^5}\right) \tag{42}$$

The analytic solution for concentration is obtained by solving the Eq. (12). The solution is given as follows,

$$\sigma = 1 + -ScSr[R_1 + AR_2 + \beta\{(1 - Q_2)R_1 + R_3\} + A\beta\{-AQ_{12}R_1 + (1 - Q_2)R_2 + R_4\}] + ScSr[R_5 + AR_6 + \beta\{(1 - Q_2)R_5 + R_7\} + A\beta\{-Q_{12}R_5 + (1 - Q_2)R_6 + R_8\}] \tag{43}$$

4. Results and Discussions

The present section is to comprehend and analyse how different parameters affect the Eyring Powell fluid flow in a peristaltic channel under the influence of heat and mass transfer as well as variable liquid properties. The results of the analysis for velocity, temperature, concentration, and stream function are represented graphically.

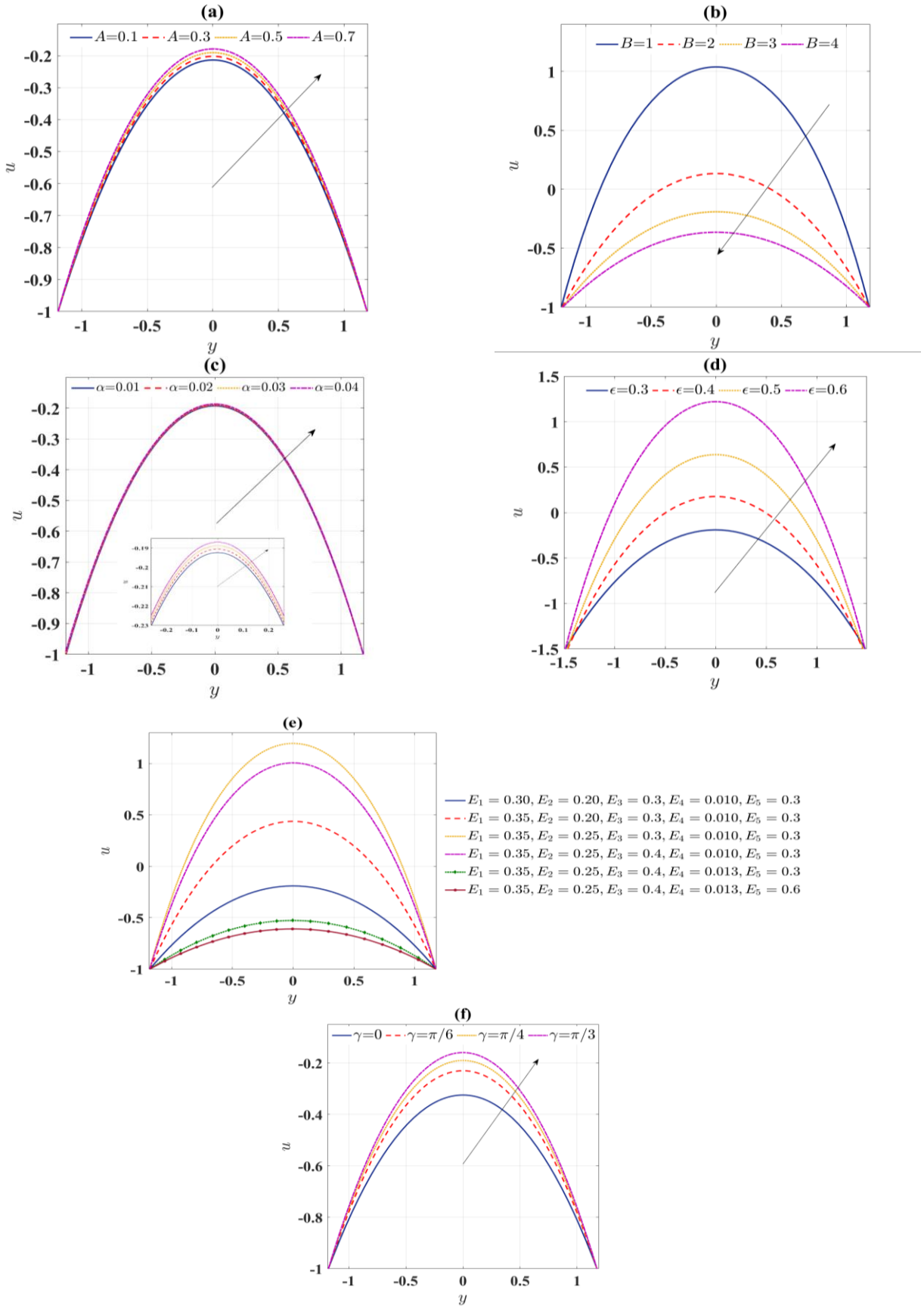

Fig. 2. Variation of velocity profiles when E_1= 0.3, E_2= 0.2, E_3= 0.3, E_4= 0.01, E_5= 0.3, A=0.5, B=3, x= 0.2, F= 1, $\gamma = \frac{\pi}{4}$, α = 0.02, t=0.1, $\epsilon = 0.3$

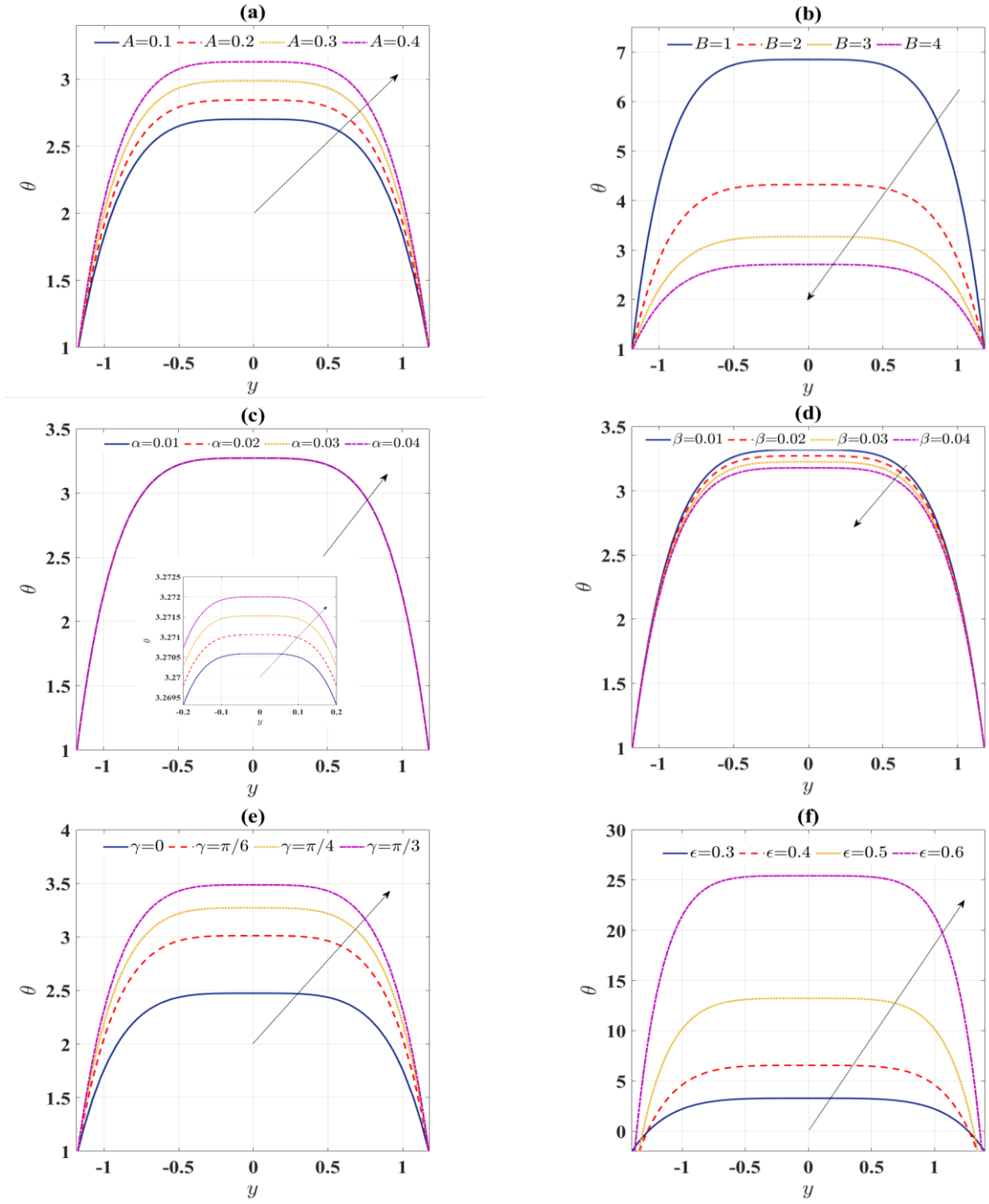
(a)
A=0.1
A=0.2
A=0.3
A=0.4
θ
y
(b)
B=1
B=2
B=3
B=4
θ
y
(c)
α=0.01
α=0.02
α=0.03
α=0.04
θ
y
(d)
β=0.01
β=0.02
β=0.03
β=0.04
θ
y
(e)
γ=0
γ=π/6
γ=π/4
γ=π/3
θ
y
(f)
ϵ=0.3
ϵ=0.4
ϵ=0.5
ϵ=0.6
θ
y

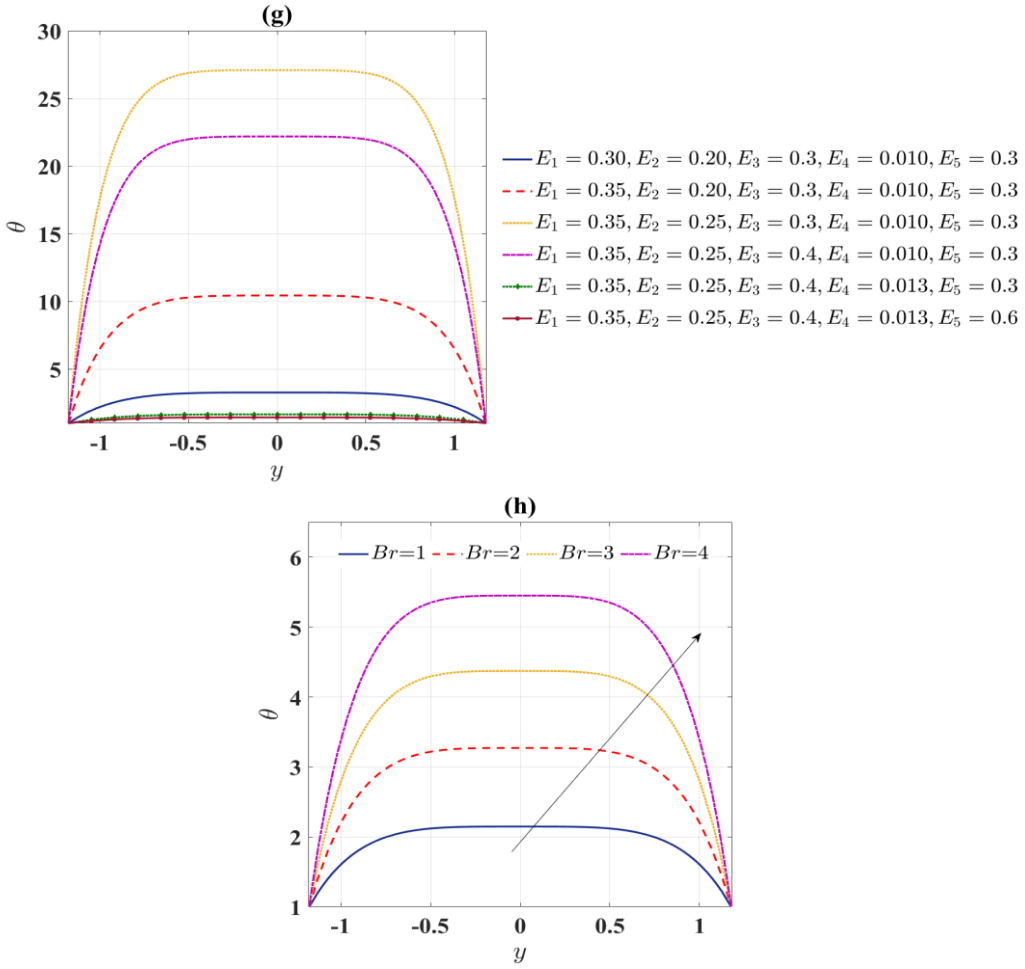

Fig. 3. Variation of temperature profiles when E_1= 0.3, E_2= 0.2, E_3= 0.3, E_4= 0.01, E_5= 0.3, A=0.5, B=3, x= 0.2, F= 1, $\gamma = \frac{\pi}{4}$, α = 0.02, β =0.02, t=0.1, $\epsilon = 0.3$, Br=2

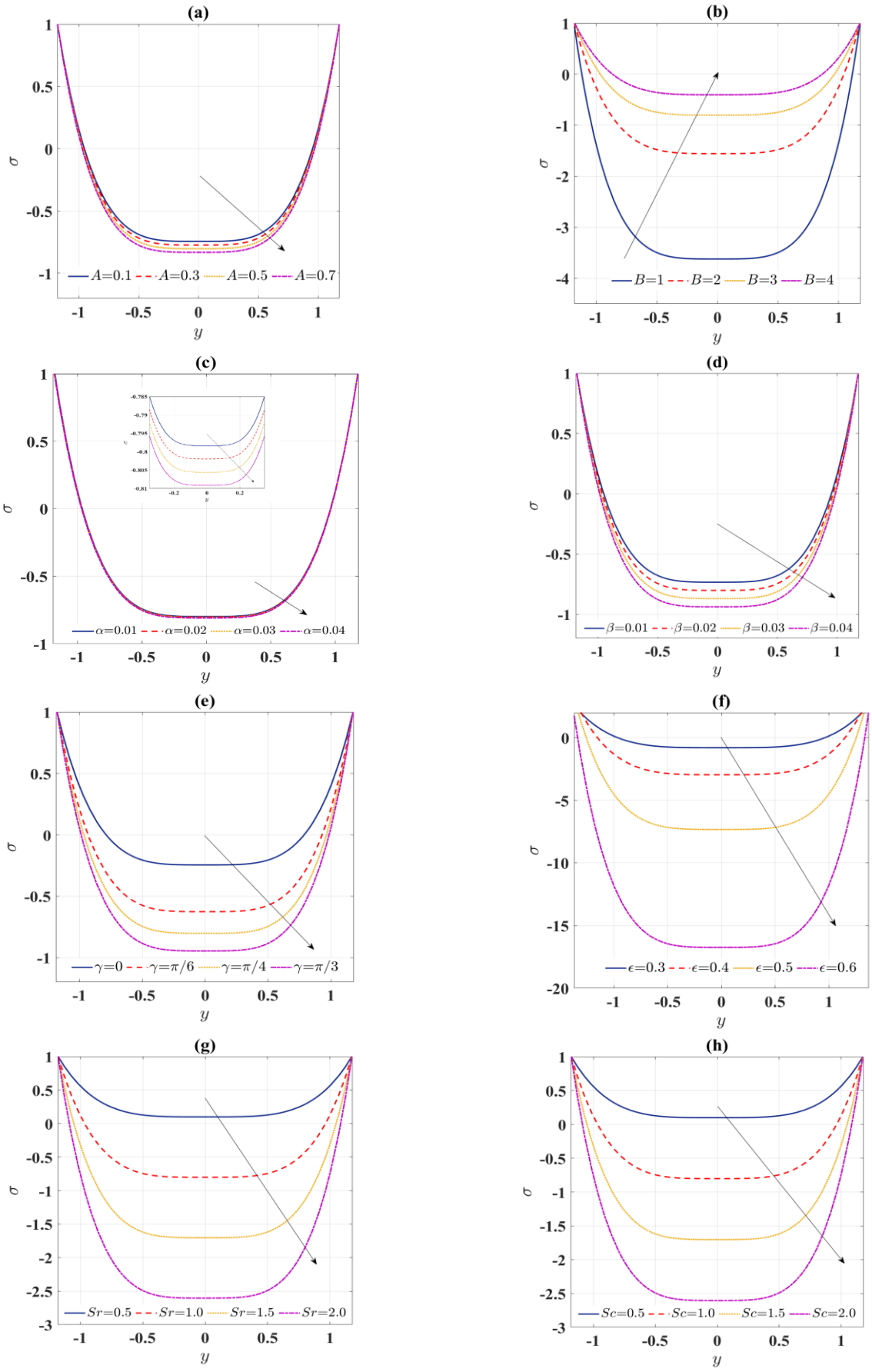
(a)
A=0.1 A=0.3 A=0.5 A=0.7
(b)
B=1 B=2 B=3 B=4
(c)
α=0.01 α=0.02 α=0.03 α=0.04
(d)
β=0.01 β=0.02 β=0.03 β=0.04
(e)
γ=0 γ=π/6 γ=π/4 γ=π/3
(f)
ϵ=0.3 ϵ=0.4 ϵ=0.5 ϵ=0.6
(g)
Sr=0.5 Sr=1.0 Sr=1.5 Sr=2.0
(h)
Sc=0.5 Sc=1.0 Sc=1.5 Sc=2.0
σ
y

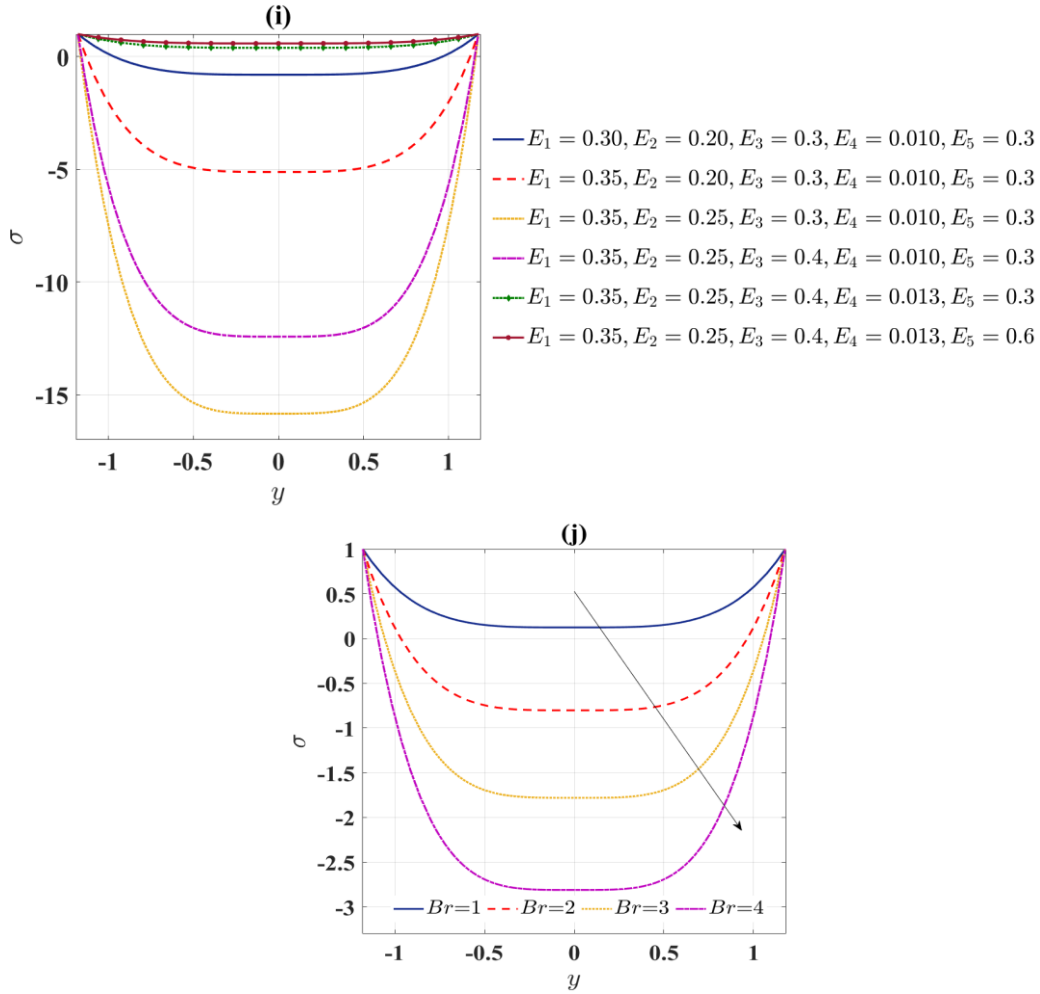

Fig. 4. Variation of concentration profiles when E_1= 0.3, E_2= 0.2, E_3= 0.3, E_4= 0.01, E_5 = 0.3, A=0.5, B =3, x = 0.2, F = 1, $\gamma = \frac{\pi}{4}$, α = 0.02, β=0.02, t=0.1, $\epsilon = 0.3$, Br =2, Sc =1, Sr =1

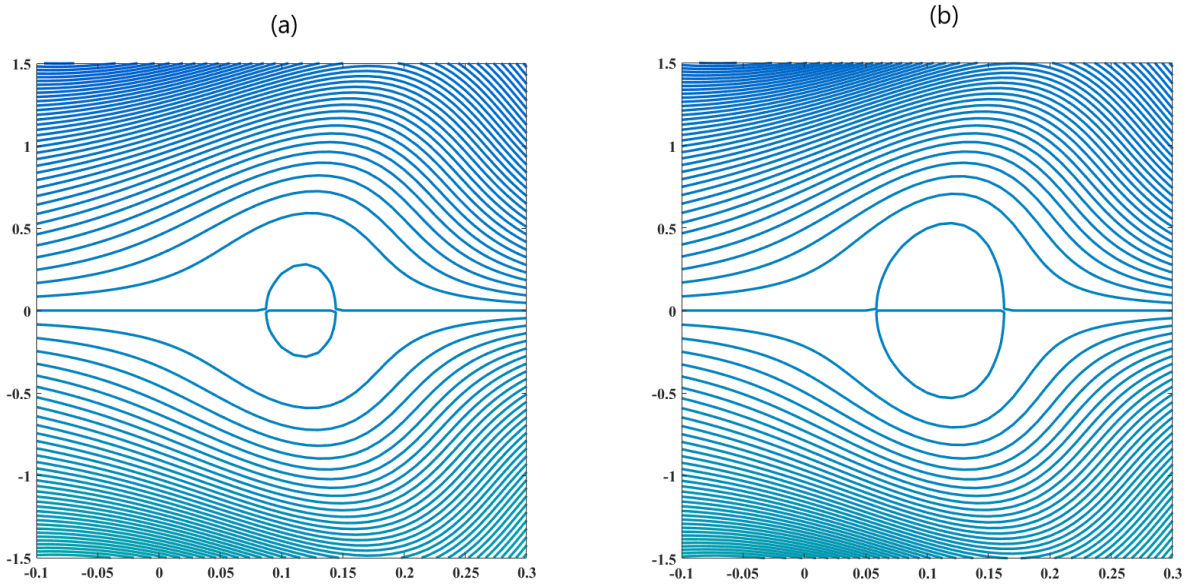

Fig. 5. Variation of streamlines for (a) A=0.1 and (b) A= 0.5

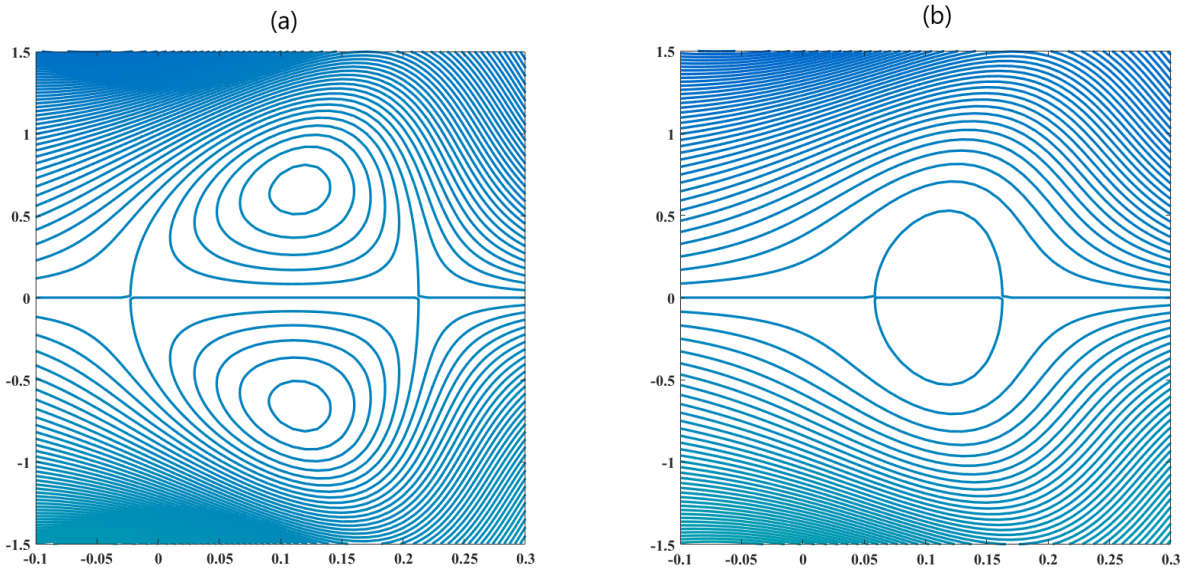

Fig. 6. Variation of streamlines for (a) B=2 and (b) B= 3

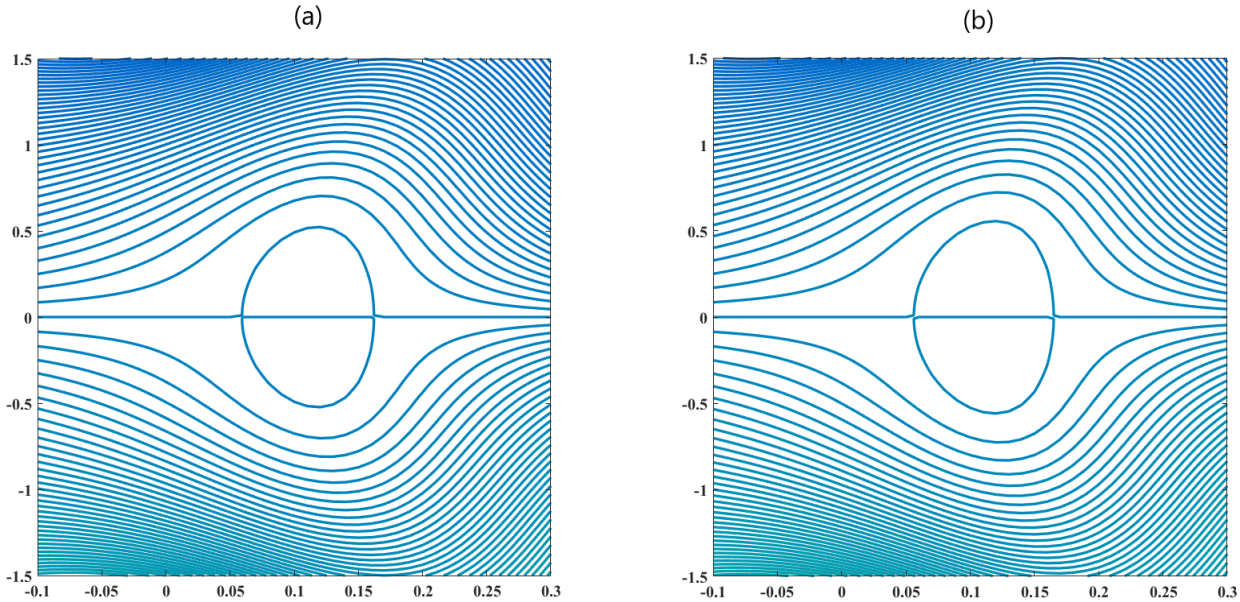

Fig. 7. Variation of streamlines for (a) α =0.01 and (b) α = 0.06

(a)

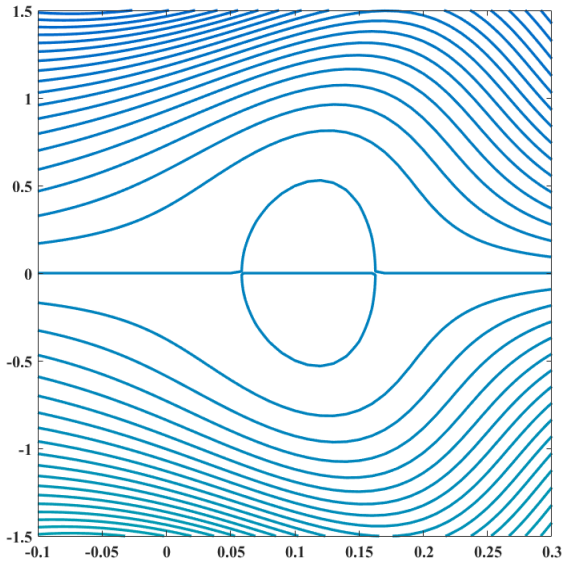
1.5
1
0.5
0
-0.5
-1
-1.5
-0.1
-0.05
0
0.05
0.1
0.15
0.2
0.25
0.3

(b)

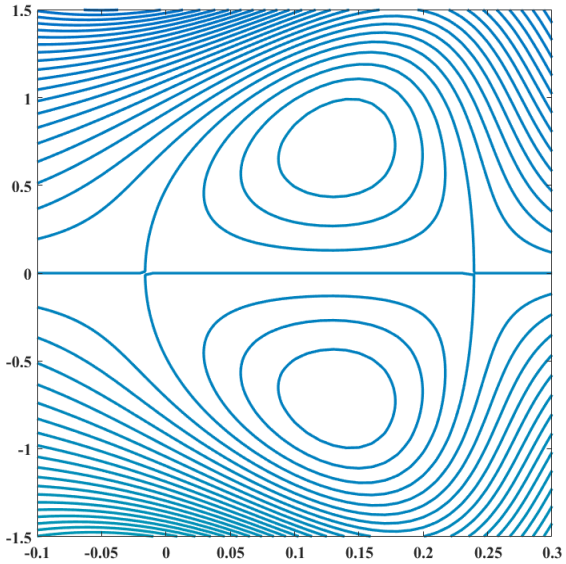
1.5
1
0.5
0
-0.5
-1
-1.5
-0.1
-0.05
0
0.05
0.1
0.15
0.2
0.25
0.3

(c)

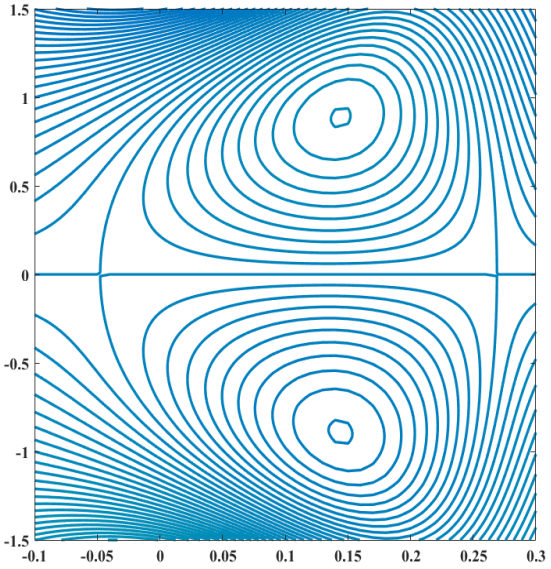
1.5
1
0.5
0
-0.5
-1
-1.5
-0.1
-0.05
0
0.05
0.1
0.15
0.2
0.25
0.3

(d)

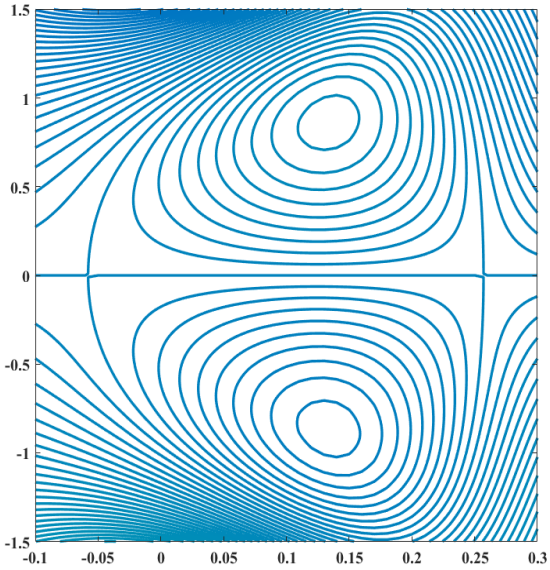
1.5
1
0.5
0
-0.5
-1
-1.5
-0.1
-0.05
0
0.05
0.1
0.15
0.2
0.25
0.3

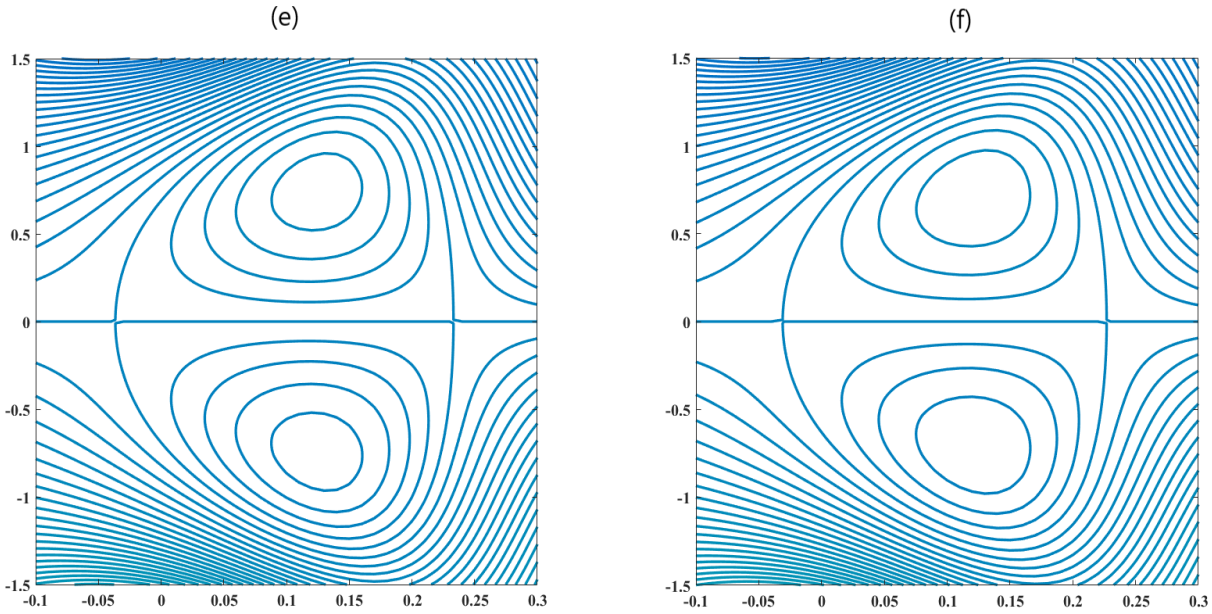

Fig. 8. Variation of streamlines for (a) $E_1 = 0.3, E_2 = 0.2, E_3 = 0.3, E_4 = 0.01, E_5 = 0.3$; (b) $E_1 = 0.35, E_2 = 0.2, E_3 = 0.3, E_4 = 0.01, E_5 = 0.3$; (c) $E_1 = 0.35, E_2 = 0.25, E_3 = 0.4, E_4 = 0.01, E_5 = 0.3$; (d) $E_1 = 0.35, E_2 = 0.25, E_3 = 0.4, E_4 = 0.01, E_5 = 0.3$; (e) $E_1 = 0.35, E_2 = 0.25, E_3 = 0.4, E_4 = 0.011, E_5 = 0.3$; (f) $E_1 = 0.35, E_2 = 0.25, E_3 = 0.4, E_4 = 0.011, E_5 = 0.6$.

4.1 Velocity Profiles

The importance of this section is to analyze the impact of velocity profiles with varying pertinent parameters Figure 2(a)-(f) has been sketched to analyze the effects of variation of material parameters, variable viscosity, amplitude ratio variable thermal conductivity, wall properties and angle of inclination on velocity. Figure 2(a)-(b) has drawn to analyze the fluid parameter of the Eyring Powell fluid on velocity. The graph shows that as the fluid parameter A increases, the velocity profile also increases. An opposite trend is seen in case of fluid parameter B. For an increase in variable viscosity, the rise in velocity profiles has been noticed (See Figure 2(c)). Figure 2(d) shows that the variation of velocity for amplitude ratio. The velocity profile improves with the larger value of the amplitude ratio. Figure 2(e) indicated the change in velocity due to varying wall properties. An increase in velocity can be seen for an increase in wall tension and mass characterization parameters but as the wall damping parameter increases, the velocity profiles diminish. A minute change in the wall rigidity parameter diminishes the velocity greatly. Similar behavior is seen for the wall elasticity parameter. An increase in the elasticity parameter decreases the velocity profile. Figure 2(f) represents the variation in the inclination angle, which improves the velocity profile for higher values of the angle of inclination.

4.2 Temperature Profiles

The present section emphasizes the effect of diverse parameters such as temperature profiles with varying pertinent parameters such as variation of material parameters, variable viscosity, amplitude ratio, variable thermal conductivity, wall properties and angle of inclination on temperature represented in Figures 3(a)-(h). Figures 3(a)-(b) show the effect of fluid parameters A and B on temperature. It has been noticed that an increase in fluid parameter A increases the temperature profiles, and a rise in liquid parameter B decreases the temperature. Figure 3(c)-(d)

shows that an increase in the coefficient of variable viscosity increases the temperature while the rise in variable thermal conductivity reduces the temperature. Figures 3(e)-(f) are sketched to analyze the temperature variation for the angle of inclination and amplitude ratio. They show similar behavior for temperature i.e., rise in both inclination angle and amplitude ratio improves the temperature profiles. Figure 3(g) has been drawn for varying wall properties on temperature. An increase in the wall tension and mass characterization parameter increases the temperature while the damping parameter shows opposite behavior. Rise in the wall damping parameter and rigidity parameter decreases the temperature profiles. A negligible decrease has seen in the rise of the wall elasticity parameter. An enhancement in temperature profiles is seen for the increase in Brinkmann number (See Figure 3(h)).

4.3 Concentration Profiles

This section explains the effect of significant parameters on the concentration profiles is depicted in Figure 4(a)-(j) represents varying parameters on concentration. Figure 4(a)-(b) shows the effects of Eyring-Powell parameters A and B on concentration, the Eyring-Powell parameters A decreases the concentration profile while the increase in liquid parameter B has an opposite impact on the concentration profile. Figure 4(c) shows lower the concentration for the higher value of variable viscosity. Similar behavior is seen in the case of variable thermal conductivity (See Figure 4(d)). Figures 4(e)-(h) has been sketched to analyze the variation of inclination angle, amplitude ratio, Soret number and Schmidt number on concentration. It has been noticed that for increasing all these parameters decreases the concentration profiles. Figure 4(i) is plotted for the variation of concentration on wall properties. A decrease in concentration profile is seen for an increase in wall tension and mass characterization parameter. This behavior is opposite to that in velocity and temperature profiles. As the wall damping parameter increases, the concentration profiles notice a huge enhancement. Similar behavior is seen in the case of the wall rigidity parameter. The Wall elasticity parameter improves the concentration profile. Figure 4(j) shows the decrease in concentration profile for a rise in Brinkmann number.

4.4 Trapping Phenomenon

The trapping is an important phenomenon in analyzing the peristaltic mechanism of biological liquids because it shows boluses' formation through closed streamlines. These streamlines are plotted in Figure 5-8. Figure 5 interprets streamlines' variation for different values of fluid parameter A. The size of the bolus has increased from $A = 0.1$ to $A = 0.5$. In Figure 6 The opposite behavior is seen in liquid parameter B. The number of boluses decreases for an increase value from $B = 2$ to $B = 3$. Figure 7 depicts the streamlines for variation of coefficient of variable viscosity. As variable viscosity increases, the bolus size increases. Figure 8(a) shows that effect of wall properties on streamlines. It can be noticed that as the wall tension parameter increases, there is an increase in the size of the bolus. Figure 8(b)- (c) shows the number of bolus increases. It is due to the rise in mass characterization parameters. Figure 8(d) revels that the size of the bolus decrease with an increase in the wall damping parameter. Similar behavior is seen in Figure 8(e), as the increased rigidity of the wall, decreases the number of boluses. Figure 8(f) shows the size of the boluses has reduced for an increase in the wall elasticity parameter.

5. Validation of the Results

The obtained solutions satisfy both the required boundary conditions and the dimensionless governing equations perfectly. The streamline, temperature, and concentration solutions obtained by Eq. (30), (36) and (43) respectively, are in accordance with the boundary conditions given in Eq. (15), and we obtain ψ = - 1, ϑ = 1, and σ = 1 as specified in boundary conditions (15). These equations are also satisfied if the solutions provided by Eq. (30), (36) and (43) are substituted into Eq. (9-12). The given solutions therefore satisfy all governing equations and requirements. Furthermore, the graphical solutions provide appropriate representations of the flow profile based on the simulated problem, which serves to confirm the boundary conditions for this flow that were considered. The results are further supported by Hina's [31] work when in the absence of MHD, and no-slip condition. The outcomes are consistent even in the absence of variable liquid properties.

6. Conclusions

An Eyring-Powell fluid peristaltic process is examined in a uniform channel with convective boundary conditions and varying liquid characteristics. Small quantities of variable viscosity and heat conductivity may be modelled using the semi-analytical approach (double perturbation). Analytical methods are used to discover the values of velocity and concentration. Some crucial findings from the present model are

i. In terms of velocity, temperature, concentration, and streamline functions, the Eyring-Powell fluid parameters A and B behave oppositely.
ii. The wall properties E_1 and E_2 increase the velocity and temperature while E_3, E_4 and E_5 decrease the velocity and temperature profiles. Opposing behavior can be seen in the concentration profile.
iii. While the concentration is reduced, the velocity and temperature profiles are increased for inclination angle.
iv. Variable thermal conductivity decreases for both temperature and concentration profiles. Brinkmann number increases the temperature during the peristalsis.
v. The variable viscosity increases, the bolus size increases.

Acknowledgement
This research was not funded by any grant.

References

[1] Latham, Thomas Walker. "Fluid motions in a peristaltic pump." PhD diss., Massachusetts Institute of Technology, 1966.
[2] Shapiro, Ascher H., Michel Yves Jaffrin, and Steven Louis Weinberg. "Peristaltic pumping with long wavelengths at low Reynolds number." *Journal of fluid mechanics* 37, no. 4 (1969): 799-825. https://doi.org/10.1017/S0022112069000899
[3] Raju, K. Kanaka, and Rathna Devanathan. "Peristaltic motion of a non-Newtonian fluid." *Rheologica Acta* 11, no. 2 (1972): 170-178. https://doi.org/10.1007/BF01993016
[4] Srivastava, L. M., V. P. Srivastava, and S. N. Sinha. "Peristaltic transport of a physiological fluid." *Biorheology* 20, no. 2 (1983): 153-166. https://doi.org/10.3233/BIR-1983-20205
[5] Usha, S., and A. Ramachandra Rao. "Peristaltic transport of two-layered power-law fluids." (1997): 483-488. https://doi.org/10.1115/1.2798297

[6] Vajravelu, K., S. Sreenadh, and V. Ramesh Babu. "Peristaltic pumping of a Herschel–Bulkley fluid in a channel." *Applied Mathematics and Computation* 169, no. 1 (2005): 726-735. https://doi.org/10.1016/j.amc.2004.09.063
[7] Hayat, T., Naseema Aslam, A. Alsaedi, and M. Rafiq. "Numerical analysis for endoscope and Soret and Dufour effects on peristalsis of Prandtl fluid." *Results in physics* 7 (2017): 2855-2864. https://doi.org/10.1016/j.rinp.2017.07.058
[8] Hayat, T., Naseema Aslam, Ahmed Alsaedi, and M. Rafiq. "Endoscopic effect in MHD peristaltic activity of hyperbolic tangent nanofluid: a numerical study." *International Journal of Heat and Mass Transfer* 115 (2017): 1033-1042. https://doi.org/10.1016/j.ijheatmasstransfer.2017.07.110
[9] Vaidya, Hanumesh, C. Rajashekhar, G. Manjunatha, and K. V. Prasad. "Peristaltic mechanism of a Rabinowitsch fluid in an inclined channel with complaint wall and variable liquid properties." *Journal of the Brazilian Society of Mechanical Sciences and Engineering* 41 (2019): 1-14. https://doi.org/10.1007/s40430-018-1543-4
[10] Sobh, Ayman Mahmoud. "Heat transfer in a slip flow of peristaltic transport of a magneto-Newtonian fluid through a porous medium." *International Journal of Biomathematics* 2, no. 03 (2009): 299-309. https://doi.org/10.1142/S1793524509000704
[11] Ali, Nasir, M. Sajid, Tariq Javed, and Zaheer Abbas. "Heat transfer analysis of peristaltic flow in a curved channel." *International Journal of Heat and Mass Transfer* 53, no. 15-16 (2010): 3319-3325. https://doi.org/10.1016/j.ijheatmasstransfer.2010.02.036
[12] Alsaedi, A., Naheed Batool, H. Yasmin, and T. Hayat. "Convective heat transfer analysis on Prandtl fluid model with peristalsis." *Applied Bionics and Biomechanics* 10, no. 4 (2013): 197-208. https://doi.org/10.1155/2013/920276
[13] Bhatti, M. M., and A. Zeeshan. "Heat and mass transfer analysis on peristaltic flow of particle–fluid suspension with slip effects." *Journal of Mechanics in Medicine and Biology* 17, no. 02 (2017): 1750028. https://doi.org/10.1142/S0219519417500282
[14] Vaidya, Hanumesh, C. Rajashekhar, G. Manjunatha, K. V. Prasad, O. D. Makinde, and K. Vajravelu. "Heat and mass transfer analysis of MHD peristaltic flow through a complaint porous channel with variable thermal conductivity." *Physica Scripta* 95, no. 4 (2020): 045219. https://doi.org/10.1088/1402-4896/ab681a
[15] Manjunatha, G., C. Rajashekhar, Hanumesh Vaidya, K. V. Prasad, and B. B. Divya. "Heat transfer analysis on peristaltic transport of a Jeffery fluid in an inclined elastic tube with porous walls." *International Journal of Thermofluid Science and Technology* 7, no. 1 (2020): 20070101. https://doi.org/10.36963/IJTST.20070101
[16] Gurrampati, Venkata Ramana Reddy. "Cattaneo-Christov Heat and Mass Transfer Flux Across Electro-Hydrodynamics Blood-Based Hybrid NanoFluid Subject to Lorentz Force." *CFD Letters* 14, no. 7 (2022): 124-134. https://doi.org/10.37934/cfdl.14.7.124134
[17] Kothandapani, M., and S. Srinivas. "On the influence of wall properties in the MHD peristaltic transport with heat transfer and porous medium." *Physics letters A* 372, no. 25 (2008): 4586-4591. Hayat, T., and S. Hina. "The influence of wall properties on the MHD peristaltic flow of a Maxwell fluid with heat and mass transfer." *Nonlinear analysis: Real world applications* 11, no. 4 (2010): 3155-3169. https://doi.org/10.1016/j.physleta.2008.04.050
[18] Javed, Maryiam, Tasawar Hayat, and A. Alsaedi. "Effect of wall properties on the peristaltic flow of a non-Newtonian fluid." *Applied Bionics and Biomechanics* 11, no. 4 (2014): 207-219. https://doi.org/10.1155/2014/802361
[19] Devaki, P., S. Sreenadh, K. Vajravelu, K. V. Prasad, and Hanumesh Vaidya. "Wall properties and slip consequences on peristaltic transport of a casson liquid in a flexible channel with heat transfer." *Applied Mathematics and Nonlinear Sciences* 3, no. 1 (2018): 277-290. https://doi.org/10.21042/AMNS.2018.1.00021
[20] Manjunatha, Gudekote, Choudhari Rajashekhar, Hanumesh Vaidya, K. V. Prasad, and Oluwole Daniel Makinde. "Effects wall properties on peristaltic transport of rabinowitsch fluid through an inclined non-uniform slippery tube." In *Defect and Diffusion Forum*, vol. 392, pp. 138-157. Trans Tech Publications Ltd, 2019. https://doi.org/10.4028/www.scientific.net/DDF.392.138
[21] Rajashekhar, C., G. Manjunatha, Hanumesh Vaidya, B. Divya, and K. Prasad. "Peristaltic flow of Casson liquid in an inclined porous tube with convective boundary conditions and variable liquid properties." *Frontiers in Heat and Mass Transfer (FHMT)* 11 (2018). https://doi.org/10.5098/hmt.11.35
[22] Vaidya, Hanumesh, Rajashekhar Choudhari, Manjunatha Gudekote, and Kerehalli Vinayaka Prasad. "Effect of variable liquid properties on peristaltic transport of Rabinowitsch liquid in convectively heated complaint porous channel." *Journal of Central South University* 26, no. 5 (2019): 1116-1132. https://doi.org/10.1007/s11771-019-4075-x
[23] Vaidya, Hanumesh, C. Rajashekhar, Manjunatha Gudekote, Kerehalli Vinayaka Prasad, Oluwole Daniel Makinde, and S. Sreenadh. "Peristaltic motion of non-newtonian fluid with variable liquid properties in a convectively heated nonuniform tube: Rabinowitsch fluid model." *Journal of Enhanced Heat Transfer* 26, no. 3 (2019). https://doi.org/10.1615/JEnhHeatTransf.2019029230
[24] Manjunatha, G., C. Rajashekhar, Hanumesh Vaidya, K. V. Prasad, and K. Vajravelu. "Impact of heat and mass transfer on the peristaltic mechanism of Jeffery fluid in a non-uniform porous channel with variable viscosity and thermal

conductivity." *Journal of Thermal Analysis and Calorimetry* 139 (2020): 1213-1228. https://doi.org/10.1007/s10973-019-08527-8

[25] Vaidya, Hanumesh, C. Rajashekhar, G. Manjunatha, K. V. Prasad, O. D. Makinde, and K. Vajravelu. "Heat and mass transfer analysis of MHD peristaltic flow through a complaint porous channel with variable thermal conductivity." *Physica Scripta* 95, no. 4 (2020): 045219. https://doi.org/10.1088/1402-4896/ab681a

[26] Divya, B. B., G. Manjunatha, C. Rajashekhar, Hanumesh Vaidya, and K. V. Prasad. "Analysis of temperature dependent properties of a peristaltic MHD flow in a non-uniform channel: a Casson fluid model." *Ain Shams Engineering Journal* 12, no. 2 (2021): 2181-2191. https://doi.org/10.1016/j.asej.2020.11.010

[27] Rajashekhar, C., F. Mebarek-Oudina, Hanumesh Vaidya, K. V. Prasad, G. Manjunatha, and H. Balachandra. "Mass and heat transport impact on the peristaltic flow of a Ree–Eyring liquid through variable properties for hemodynamic flow." *Heat Transfer* 50, no. 5 (2021): 5106-5122. https://doi.org/10.1002/htj.22117

[28] Vaidya, Hanumesh, Rajashekhar Choudhari, Fateh Mebarek-Oudina, Isaac Lare Animasaun, Kerehalli Vinayaka Prasad, and Oluwale Daniel Makinde. "Combined effects of homogeneous and heterogeneous reactions on peristalsis of Ree-Eyring liquid: Application in hemodynamic flow." *Heat Transfer* 50, no. 3 (2021): 2592-2609. https://doi.org/10.1002/htj.21995

[29] Ewis, Karem Mahmoud. "Effects of Variable Thermal Conductivity and Grashof Number on Non-Darcian Natural Convection Flow of Viscoelastic Fluids with Non Linear Radiation and Dissipations." *Journal of Advanced Research in Applied Sciences and Engineering Technology* 22, no. 1 (2021): 69-80. https://doi.org/10.37934/araset.22.1.6980

[30] Akbar, Noreen Sher, and S. Nadeem. "Characteristics of heating scheme and mass transfer on the peristaltic flow for an Eyring–Powell fluid in an endoscope." *International Journal of Heat and Mass Transfer* 55, no. 1-3 (2012): 375-383. https://doi.org/10.1016/j.ijheatmasstransfer.2011.09.029

[31] Noreen, S., and M. Qasim. "Peristaltic flow of MHD Eyring-Powell fluid in a channel." *The European Physical Journal Plus* 128 (2013): 1-10. https://doi.org/10.1140/epjp/i2013-13091-3

[32] Hina, S. "MHD peristaltic transport of Eyring–Powell fluid with heat/mass transfer, wall properties and slip conditions." *Journal of Magnetism and Magnetic Materials* 404 (2016): 148-158. https://doi.org/10.1016/j.jmmm.2015.11.059

[33] Farooq, S., T. Hayat, B. Ahmad, and A. Alsaedi. "MHD flow of Eyring–Powell liquid in convectively curved configuration." *Journal of the Brazilian Society of Mechanical Sciences and Engineering* 40 (2018): 1-14. https://doi.org/10.1007/s40430-018-1071-2

[34] Mabood, Fazle, W. Farooq, and A. Abbasi. "Entropy generation analysis in the electro-osmosis-modulated peristaltic flow of Eyring–Powell fluid." *Journal of Thermal Analysis and Calorimetry* (2022): 1-16.

[35] Kotnurkar, Asha, and Namrata Kallolikar. "Effect of Surface Roughness and Induced Magnetic Field on Electro-Osmosis Peristaltic Flow of Eyring Powell Nanofluid in a Tapered Asymmetric Channel." *Journal of Advanced Research in Numerical Heat Transfer* 10, no. 1 (2022): 20-37.